On the origin and distribution of internal erosion signatures in the floodplain protected by river dikes

Laurence Girolami, Stéphane Bonelli, Jean-Michel Carozza, Edouardo-Jovick Fogueng-Wafo, Jules Burgat, Naïm Chaouch, Rémi Valois

On the origin and distribution of internal erosion signatures in the floodplain protected by river dikes

Laurence Girolami[1,2], Stéphane Bonelli[1], Jean-Michel Carozza[3], Edouardo-Jovick Fogueng-Wafo[1], Jules Burgat[1], Naïm Chaouch[1], Rémi Valois[4]

[1] INRAE Aix-Marseille Université UMR RECOVER, Aix-en-Provence, France

[2] GéHCO, Campus Grandmont, Université de Tours, Tours, France

[3] LIENSs, CNRS-UMR, Department of Human and Social Sciences, La Rochelle University, La Rochelle, France

[4] INRAE Université d'Avignon UMR EMMAH, Avignon, France

Corresponding author: Laurence Girolami; E-mail: laurence.girolami@inrae.fr

Abstract

The subsoils of river dikes are often composed of highly permeable and low-density river sediments. Thus, erosion signatures (leaks, sand boils, sinkholes) can appear in the protected floodplain during floods, highlighting the development of hydromorphodynamic phenomena below the surface, which may harm the safety of the dike system. A multi-scale methodology is deployed to understand and analyze the influence of floodplain architecture in terms of geological formations on the appearance of local erosion signatures. Particular attention is paid to the morphology of paleovalleys and paleochannels, in order to image the subsurface in terms of substrate types and interfaces using geophysical methods. This information makes it possible to propose internal erosion scenarios. Application to a study area in South of France (the Agly dike system) leads to new results. The classical backward erosion piping scheme is not relevant to explain the observed sand boils, as they are mainly caused by suffusion-type internal erosion process. Suffusion and contact erosion appear to be the origin of sinkholes. The distribution of these signatures appears to be directly related to the shape and dimensions of the paleovalley and paleochannels, as well as to the presence of a low-permeability topsoil.

Keywords

Flood protection dikes, paleovalley, alluvial terraces, paleochannels, floodplain architecture, sand boils, sinkholes, internal erosion.

1 Introduction

Globally, most low-lying estuarine and delta plains develop at the mouths of incised valleys formed during low sea levels, according to well-described mechanisms (Dalrymple, 1994). More than 158 such sites have been inventoried by Wang et al. (2019), covering low-lying areas with large, dense human populations. To ensure their safety, many rivers in these low-lying plains were dammed up, relying on the filling of these paleovalleys.

The subsoils beneath these dikes and in the protected floodplain are generally made up of highly permeable, coarse-grained fluvial deposits. They are often affected by underseepage and internal erosion processes during flood periods. The surface manifestation of these underlying phenomena usually takes the form of leaks, sand boils, and sinkholes, developed at various scales (from a few centimeters to a few tens of meters; Figure 1), all along the dikes, and not too far from them (Figure 2) (Semmens and Zhou, 2019; Marchi et al., 2021; Girolami et al., 2023). However, there is still a lack of in situ observations to track the spatio-temporal evolution of the various processes involved at different scales, so the question of their origin and distribution is not well understood or reliably described in the literature (Bonelli, 2012; 2013; Van et al., 2022). Despite the importance of this topic in terms of risk analysis, there is still a lack of studies devoted to mapping flood risks associated with artesian conditions and topsoil uplifts the protected zone (Julinek et al., 2020; Michelazzo et al. 2018).

The safety of a dike is influenced by small-scale defects (Ceccato and Simonini, 2023), which requires a good understanding of internal flows (Camici et al., 2017). Similarly, the location of leaks, sand boils and sinkholes is significantly influenced by the nature of the geological formations, in terms of depth and extent of the permeable layers formed by the presence of paleovalleys or paleochannels (Kolb, 1975; Wolff, 2002; Pazzi et al., 2018; Semmens and Zhou, 2019). A correct analysis of the flow beneath the dike requires a description of the subsurface geology, in plan and profile. Geophysical methods provide this type of information, and are used for dike systems (CIRIA, 2013; USBR, 2019; Dezert et al., 2019). Here we consider the following general situation: the paleovalley contains permeable fluvial sediments, which represent unconsolidated superficial soils (sand and gravels), overlying a marly basement of low permeability. The bedrock, located at large depth, is not considered. Interfaces between paleovalley topography and paleochannel fill and marly bedrock are investigated. Contrasts are more likely to be marked in terms of electrical properties than elastic moduli. For these reasons, electrical and electromagnetic methods are preferred. This combination is particularly effective for mapping superficial decompaction layers (Valois et al., 2011). Combined with sediment cores analyzed in the laboratory, the electrical measurements can then be converted into a geological map at a depth of several tens of meters (Mouhri et al., 2013; Chavez Olalla et al., 2022). Hydraulic conductivities can then be determined using conventional geotechnical correlations based on effective grain size.

The aim of this study is to take a step towards establishing a link, beyond the state of the art (CIRIA, 2013; USBR, 2019), between sedimentary architecture (geometry of the layers, nature of contacts between layers and granulometric contrasts) and the associated consequences in terms of leaks, sand boils and sinkholes. The study area is located in the South of France and concerns the Agly river dike system, where numerous leaks, sand boils and sinkholes have been observed (Zwanenburg et al., 2018; Tourment et al., 2018; Van et al., 2022). The results obtained by Girolami et al. (2023), using two classical geophysical methods (Frequency Domain Electromagnetic (FDEM) and Electrical Resistivity Tomography (ERT)), show that it is not enough to conclude that backward erosion piping has occured, but that the possibility of suffusion and contact erosion must also be considered. This analysis is pursued here with a multi-scale approach to support conclusions on the origin of the signatures while obtaining new results on their distribution.

The article is organized as follows: Section 2 covers the geological and geomorphological story of the River Agly, including a description of the stratigraphic architecture of the river and its alluvial plain. Section 3 deals with erosion signatures around the dikes. Section 4 describes the results of the observation of the subsoils supporting the Agly dikes, using both frequency domain electromagnetism (FDEM) and electrical resistivity tomography (ERT), as well as examination of soil cores. Section 5 presents the four basic situations explaining the origin and distribution of erosion signatures in the floodplain protected by river dikes, in the case of a dike located on a paleovalley consisting of sandy gravels. The conclusion is the last section.

2 The geological and geomorphological history of the Agly river

Describing the morphological organization and stratigraphic architecture of the river and its alluvial plain is an important first step in correlating the sedimentary facies beneath and around the diked bed with the origin and distribution of erosion signatures that appear in the protected area during flooding events. This preliminary analysis carried out on the Agly river is subsequently used to interpret geophysical surveys enriched by examination of soil cores.

The Agly is a medium-sized river with a catchment area of 980 km^2 aligned with the E-W oriented Pyrenean compression structures. Its average flow is around 7 $m^3.s^{-1}$, and can reach up to 2,100 $m^3.s^{-1}$ during flood periods (measured at the Rivesaltes station 8 km upstream of the study area). The river drains the northern part of the Roussillon basin, a 850 km^2 triangular Oligo-Pleistocene sedimentary basin open on its eastern side to the Mediterranean Sea. Geomorphologically, the basin is divided into two main units: a narrow alluvial plain upstream, up to 2 km wide and 35 m above sea level near the town of Rivesaltes, and a coastal alluvial delta downstream, almost 6 km wide and reaching sea level between Sainte-Marie and Le Barcarès, commonly known as the Salanque plain (Figure 1).

In the basin, the thickness of the accumulated sedimentary formations can locally reach over 2,200 m (i.e. Canet borehole (Duvail et al., 2001)), while the outcropping deposits are Pliocene in age (Zanclean to Gelasian, 5.5 to 1.8 Ma). These form the tops of prograding clinoforms in a Gilbert Delta-type context (Clauzon, 1990) and are composed of fine hardened clayey-silty-sandy texture also containing limestone-type indurations in the northeastern part of the basin, which corresponds to the emerged part of the deltaic prism (i.e. alluvial plain, palustrine deposits and channel). Upstream, these formations are exposed at the surface or located beneath thin alluvial terraces ($F_{y1\text{-}3}$, F_x on Figure 1) or the recent alluvial prism and act as an impermeable bedrock (reported as Pliocene sandy marls on Figure 1).

In the Pleistocene (last 1.8 Ma), the marly substrate was eroded by the Agly river, which was braided at that time, during a glacial period (e.g. episodes of cold climate and low sea levels associated with pair marine isotopic stages (Rabineau, 2001)). In this way, the Agly gradually carved out a compound incised valley, i.e. a valley resulting from several incisions/filling cycles (Labaune et al., 2010). Based on the geotechnical data and electrical measurements described in Section 4, this paleovalley reaches a maximum depth of almost 60 m at the present-day coastline (near the town of Le Barcarès; Figure 3), while tapering upstream with a depth of around 25 m near Claira and the study area (Figure 3),which rapidly decreases and disappears near Rivesaltes where it gives way to a classic strath terrace landform (see F_{ya} and F_{yb} terraces elevated at 10-14 m above the channel respectively (Calvet, 1996); Figures 1 and 3). The incised valley was then filled by alluvial deposits forming a prograding prism through three stacked transgressive sedimentary cycles (Figures 3) showing alternating levels of pebbles and gravels (channel facies) and sands and silts (alluvial plain facies) (Aunay, 2007; Duvail, 2008). The age of these formations remains uncertain, with the exception of the latest cycle dated by the Le Barcarès borehole to the Early Holocene (i.e. 13.1-13.2 ky BP) (Tesson et al., 2005), while the main construction phase ended after the Late Middle Ages (0.5 ky BP) (Carozza et al., 2013). Sedimentary filling has significantly reduced the average slope of the plain, which ranged from 1.8 to 4 $m.km^{-1}$ during the Pleistocene to 0.7 to 1.8 $m.km^{-1}$ today. As a result, the most recent formations dating from the Late Holocene (i.e. last millennium) have overflowed the edges of the incised valley, covering the alluvial terraces located downstream of Claira (Figure 1).

The broadening of deposits, from a confined continental plain to a wide coastal fan, is associated with modification of fluvial dynamics, dominated by defluviations, crevasses and overflowing. These processes can isolate paleochannels or crevasse outcrops in the alluvial plain through thick sinuous or rectilinear permeable layers of cobbles, gravels, and sands whose permeability is significantly higher than that of the marl substrate considered impermeable. The morphology of these permeable layers, and more specifically their aspect ratio a (defined as the ratio between their width and thickness), means that they can be considered as the result from bank failure processes (Friends et al., 1979). In this classification, thin, extensive layers of a>15 consisting of poorly confined and interbedded sands and sandy silts, described as sheets, are interpreted as the signature of crevasse splays (Miall, 1996). The thick, channelized and sparsely distributed layers of a<15 layers of sands and gravels, known as ribbons, are interpreted as crevasse channels (Miall, 1996). Otherwise, extensive, heterogeneous and confined layers of a>30 consisting of thick, widespread and obliquely stratified gravels and pebbles are called paleochannels. The chronology of these defluviations is well documented for the last two millennia (Carozza et al., 2013). The accumulation of coarse sandy-gravel deposits near the riverbed led to the formation of natural levees, such that today Agly channel is perched at few meters above its alluvial plain. This characteristic is clearly visible downstream from Claira, where the banks of the Agly are raised 9 m above sea level, while the plain rises to 7 m above sea level (Figure 3). This morphological feature represents an important vulnerability factor, which can promote the spread of particles-laden flows down the alluvial plain during floods via overflows, defluviations, or dike breaches.

3 Hazardous erosion signatures around Agly river dikes

Erosion of the subsoil beneath and around river dikes has been a common phenomenon in many rivers for at least a few decades (e.g. Mississippi and Ohio rivers in 1991 (Morton and Olson, 2015); Mississippi river in 1993 (Li et al., 1996); Po river in 2018 (Marchi et al., 2021); among others (Zwanenburg et al., 2018; Van et al., 2022). On the Agly, erosion signatures (leaks, sand boils, and sinkholes) only appear during floods or periods of high water and are commonly recorded in the same places, as during the repeated floods of March 2013, November 2014, October 2018, January 2020, April 2020 (Zwanenburg et al., 2018; Tourment et al., 2018; Van et al., 2022). Sand boils are conical in shape, around 30 cm in diameter and have been observed along the North and South banks, usually next to the leaks, around 100 m from the dike toe (Figure 4). Otherwise, sinkholes have an approximately ellipsoidal shape and a flat base about 0.5 to 3 m long and were mainly observed near the dike toe or about 60 m away in the transverse direction (Figure 4). Figure 5 shows the signatures of erosion (leaks, sand boils, sinkholes) observed on the North bank after the flood of March, 6th 2013.

The first embankment system, dedicated to the stabilisation of the riverbed, dates back to the early 14th century (Carozza and Puig, 2011). Despite significant reinforcements carried out after the exceptional floods of 1936, 1940, and 1942, no coherent system was proposed until the 1970s. At that time, protecting dikes of 12.5 km long, 2.5 m high, and 8 to 12 m wide were built from 1969 to 1974 along the approximately 65 m wide river to protect 30,000 people from the risks incurred by floods. The dike embankment consists of silty sand and sandy loam, while a 2-meter-deep drainage spur was built downstream after the flood event of March 6, 2013. From 1977 to 2020, the dike system was exposed to 11 floods. The 1999 flood event caused a breach on the North bank, causing 35 casualties, with a peak flow of about 2,110 $m^3.s^{-1}$, while that of 2013 flood event caused a breach on the South bank, with a peak flow of about 970 $m^3.s^{-1}$.

Despite the fact that these internal erosion processes have been observed for a long time along river dikes, the scientific community still lacks a general vision, with an observation of the system at different scales. At large scales, (i.e., 13 km levee system scale and millennium scale), historical records, sedimentary drilling and large-scale measurements allow to mapping of fluvial morphology with alluvial deposits and bordered terraces (including paleochannels) along protected plains, which may constitute areas of preferential erosion. At the medium scale (i.e. at the dike section scale and at the flood scale), field observations and modeling allow to identify processes of internal hydromorphodynamic processes in the areas mainly affected during floods. At the small scale (i.e. at the erosion signature scale and at the scale of physical processes of fluid/grain coupling), laboratory experiments carried out under controlled conditions allow to provide a quantitative description of the physical mechanisms involved.

This work focuses on large- and medium-scale analyses of the river morphology and subsoils with the aim of first describing the origin and distribution of internal erosion signatures that affect the protected plains during floods. The geomorphological analyses cover an area of 13 km long (following the embankment system), 8 km wide, and 60 m deep. Both geophysical and geomechanical investigations cover an area of 1 km long and up to 1 km wide (following the most frequently observed erosion signatures) for a depth of up to 45 m. The study area is recognized as one of the most affected during floods (Figure 1), where erosion signatures, observed after the major flood event of March 6, 2013, have been reported and expose a borderline location (from 0 to 80 m from the dike toe), with a specific spatial distribution that alternates between leaks, sand boils, and sinkholes potentially guided by the morphology and topography of the field. The repeated appearance of these signatures after each flood event may suggest the possible presence of superficial, and highly permeable materials beneath this area. This was confirmed by a first observation of the subsoil (Girolami et al., 2023). Based on these preliminary results, the analysis is further developed in this work.

4 Observation of subsurface soils supporting Agly dikes

4.1 Imaging and sampling methods

Frequency domain electromagnetism (FDEM) is relevant for mapping lateral variations in apparent electrical conductivity in subsurfaces of protected floodplains. Measurements were performed with a Geonics EM31 equipment (McNeill, 1980; Frischknecht et al., 1991), with an operating frequency of 9.8 kHz. The instrument is made with a magnetic dipole transmitter and a coplanar magnetic dipole receiver with an intercoil spacing of 3.66 m. The vertical dipole configuration was chosen to maintain a satisfactory sensitivity for depths ranging from 0 to 6 m deep (depending on soil type), although the highest sensitivity corresponds to a depth of around

1.8 m below the surface (indicative values corresponding to a homogeneous environment). The survey was carried out along parallel profiles on a 2.5x2.5 m grid.

Electrical resistivity tomography (ERT) is relevant for mapping vertical variations in electrical conductivity or resistivity (Dahlin, 2001), while capturing reliable depths of layers interfaces when the materials have sufficiently high contrasts, such as sandy marls and gravelly sands. Different equipments were used: SYSCAL Pro (IRIS instruments) for the 470 m long P1 and P3 profiles with an electrode spacing of 5 m (measurements performed in spring 2024); ABEM SAS4000 for the 125-160 m long P2 and P4-P7 profiles with an electrode spacing of 1m (measurements performed in spring 2023). The apparent conductivity/resistivity inversion was performed with the ResIPY software (Blanchy et al., 2020), which provides 2D conductivity/resistivity sections with an investigation depth of approximately 10 times the electrode spacing.

Sediment cores were collected over the period from 22 to 29 April 2013, following the major flood of 6 March. The instrument used (Hydrofore 1200) consists in a mechanically welded chassis mounted on a fixed track of 6.5 m long and 2.5 m wide. The motorization includes hydraulic pumps coupled to a Perkins diesel engine of 125HP at 2,300 rpm. The investigation depth ranged from 5 m to 15 m deep, which allows the different layers located under the river dikes to be properly investigated and the conductivity measurements to be reliably interpreted.

4.2 Surface and cross-section mapping

In order to have an overview of the situation, we carried out a FDEM surface mapping of the electrical conductivity of the soil, averaged over the first 6 m beneath the surface, while covering an area of approximately 1 km along the dikes and up to 1 km in the transverse direction, except in vineyard fields where no measurements were carried out due to the presence of numerous metal stakes every meter (Figure 6).

The zones of lowest conductivity (10^{-2} S.m^{-1}) are shown in brown in Figure 6 and may correspond to the coarsest and more permeable materials. The zones of highest conductivity (2.5×10^{-2} S.m^{-1}) are shown in dark blue and may correspond to the finest and less permeable materials (Figure 6). At a first glance, it appears that the Agly dikes are bordered by large permeable zones up to 400 m wide and at least 6 m thick, throughout the explored section of approximately 1 km long. On the South bank, these layers are delimited by thick layers of fine and less permeable soils, while materials of intermediate grain-size, shown in green, predominate on the North bank. The plotting of the position of the erosion signatures on Figure 7 coincides with the delimitation of these permeable layers which seem to control their presence and even their distribution in the protected plains.

The location of the soil cores (4 on the South bank; 5 on the Sorth bank) is shown in Figure 7. Examination of the sediment cores, mainly sampled near the dike toe, reveals that the most permeable materials (shown in brown) consist mainly of gravel with a sandy matrix supported by cooble, or even pebbles, and represent channel deposits that can thicken up to 15 m below the dikes in some locations (see sample S4 in Figure 7). The coarsest deposits appear to be located near the edges of the dike while the finest are deposited towards the alluvial terraces. Conversely, the finest and least permeable materials (shown in dark blue) consist of sandy marls, clayey silts to silty clays, and represent a deep impermeable substrate with an approximate depth of 12.20 m at point S1 (Figure 7) or rising the surface upstream, near the town of Rivesaltes, or downstream, further from the dikes. In between, the layers shown in green consist mainly of sandy silts to silty sands (see the top of samples S_1 to S_9 in Figure 7) and represent crevasse deposits overlying alluvial terraces and paleochannels. The presence of numerous paleochannels (Figures 1 and 6) in the northern part may suggest that the river was progressively displaced downward in the southern part.

In order to explore in depth the geometry of the sediment reservoir (i.e. channel deposits) beneath river dikes and the depth of the paleovalley that delimits the interface between the sandy-gravelly sediments and the marly substrate, we carried out in 2024 two ERT profile across the embankment system, which was made possible by the river drought.

The profiles, whose position is reported in Figure 5 (see P1 and P3), 470 m long and 50 m deep, are shown in Figure 8. The low conductivity (or high resistivity) areas are shown in brown while the high conductivity (or low resistivity) areas are shown in dark blue, using the same colour bar and scale as the FDEM surface mapping for comparison.

The alluvium is a few meters thick under the current river bed and thickens under the dikes up to the protected floodplain: this is due to the system of braided deposits. This permeable level under the dikes and in the protected area extends to a depth of 35 m, roughly alternating between sandy silts, silty sands, coarse sands and numerous gravels from the surface to the substrate. Beneath these layers, sandy marls form a substrate of very low permeability located at a depth of around 18-20 m below the river.

On the north-eastern flanks, the permeable layer rises to the surface, approximately 25 to 35 m from the dike toe. On the south-western flank, it extends into the protected area for almost 200 m.

An significant difference between the two profiles lies in the north-eastern protected area. On profile P1, the permeable layer continues for approximately 50 m and is a few meters thick. On profile P3, the permeable layer does not extend into the protected area. These permeable layers are covered by a layer of topsoil consisting of sandy silt approximately one meter thick.

The combination of surface and vertical maps, obtained from granulometric analyses, allows the results to be interpret as highlighting the geometry of the valley composed of approximately 200 m wide and 25 m deep at this location, dug in the marly substrate, then filled by alluvial sediments through three superimposed transgressive cycles. Once the valley was filled, episodes of defluviation formed alluvial terraces that spread-out in the protected floodplains, thus containing paleochannels of few meters thick oriented in the northeast direction towards the Leucate basin (Figure 1).

Repeated electrical profiles across the 125 m long and 20 m deep northern dike (see P2 and P5 in Figure 5) allow to more accurately map the longitudinal geometry and base of the paleovalley in areas frequently affected by erosion, while a 164 m long and 20 m deep longitudinal profile along the dike (see P4 on Figure 5) allows to map its geometry in the protected area. As shown in the profile of the Salanque Figure 3, the paleovalley is slightly narrower and shallower upstream and becomes deeper and wider downstream (Figure 9), which is also highlighted by the longitudinal profile P4 whose thickness varies from 8 m to 12 m downstream in the protected plain (15 m from the dike toe). Figure 9 also shows photographs of the sedimentary borehole located on points P4 at a coarse level (with gravels and pebbles) at 5 m depth. These results suggest that the head of the watershed may have been affected upstream by successive erosion processes following past floods which in turn progressively filled the valley located downstream with flood deposits. Local variations in valley geometry can also locally control the velocity fields of internal and surface flows during floods, thus playing a role in the distribution of erosion signatures along the protected plain. The reconstruction of a grid of profiles (taking P2, P5, P6, P7 located in Figure 5) allows to locate the limit of erosion processes beyond which no more signatures are observed during floods (Figure 10).

More detailed profiles (Girolami et al., 2023) allows to highlight the presence of a thick permeable layer of at least 8 meters deep covered by a thin cohesive layer of around 1 meter thick and bordered by the marly substrate, under the sand boils zone. This configuration highlights the possibility of formation of fluidization chimneys, thanks to the presence of a superficial heterogeneous cohesive material, from which leaks and then sand boils (when erosion of the underlying sandy material is initiated) can develop from the permeable and granular layers. During floods, internal flows propagate within the Holocene sediments, from the river to the protected plain, following the sandy-marly interface until reaching the surface. The marly substrate at the edge, located in the north-eastern direction, plays an important role in the distribution of the sand boils by forming an impermeable barrier to internal flows that slows their progression toward the bottom of the protected plain and preferentially guides them towards the surface. The heterogeneous surface layer, on the other hand, prevents homogeneous fluidization of the entire soil (and the formation of a suspension (Amin et al., 2021)) by preferentially driving the flow through permeable chimneys. Sand erosion cany potentially occur during the flood peak when the drag force on the particles is high enough to fluidize them and transport them to the surface to eventually form a conical deposit.

Conversely, the presence of a thick sandy cover layer about 3 meters deep above the marly substrate several meters thick below the sinkhole area (Figure 8b) may favor the superficial collapse of the low-density and permeable layers after the flood peak. As observed from the sediment samples, the collapse appears to remain superficial and does not affect the layers located below the permeable lenses. Here again, the presence of sand boils in the same region is favored by the presence of a sufficiently thick sandy layer covered by a cohesive soil that will allow the formation of preferential flow pipes from which leaks and fluidization chimneys will develop. Their location near the dike toe may suggest a maximum flow velocity at this location, high enough to initiate fluidization and erosion of the sand.

5 Origin and distribution of internal erosion signatures in the protected floodplain

5.1 Occurrence by internal erosion of open-framework gravels in sandy gravels

Geophysical measurements reveal a non-tabular geometry of the interface between the highly permeable soil at the surface and the low permeable soil at depth. For a given geometry, in the case of a dike located above the paleovalley, the two main parameters are the presence of a cohesive topsoil and the presence of paleochannels extending into the protected floodplain. Here we consider the case of a paleovalley consisting of sandy gravels. If the dike system is subjected a flood, the subsoil is subjected to seepage. Due to the high permeability of the sandy gravel layer, the pressure losses are low and the pore pressures are high.

In the absence of topsoil, a permeable subsurface layer can lead to slow flooding of the protected area, as the water table rises through the paleovalleys.

In the presence of low-permeability topsoil, high pore pressures result, from the first flood, in the appearance of artesian zones and uplift zones in the protected area. In artesian zones, the slightest defect in the topsoil can lead to leakage (concentrated outflow of seepage water, also known as boils) in the protected area. Examples of a defect are a fluidized sand vein (heave) or a pre-existing vertical crack. In the uplift zones, the cohesive topsoil is subject to hydraulic failure (cracking).

The presence of defects in the topsoil is a triggering factor for sand boils and backward erosion. Since the soil beneath the topsoil is sandy gravel, erosion is caused by suffusion, which appears to be selective backward erosion. This process has not yet been studied to our knowledge. We propose to call it *backward erosion suffusion*. This is a different process from that generally considered to explain sand boils and their consequences. The usual assumption is that the permeable layer is sand, and that backward erosion creates a pipe under the topsoil. This is called *backward erosion piping* (van Beek et al., 2011; Bonelli, 2013).

In all case, the erosion of the sandy gravel causes the appearance of low density areas, immediately under the dike and in some places under the topsoil layer, inside the permeable layer at the level of the reduction in the thickness of the sandy gravel layer if a paleochannel exists (Deng et al., 2025; Bonelli and Girolami, 2025). This internal erosion actually transforms some areas of the sandy gravel into open-framework gravel. These are the red areas in Figure 11.

Open-framework gravel has a unimodal particle size distribution with a mean particle size greater than 2 mm (without sand), with a hydraulic conductivity above 10^{-2} m/s. Gravelly fluvial deposits contain open-framework gravel as planar and cross-strata of varying scale, usually overlain by and resting on bimodal sandy gravel (Lunt and Bridge, 2007).

The presence of open-framework gravel is an important factor in triggering internal erosion and sinkholes (Luo and Huang, 2020; Fell et al., 2014): excessively high flow rates through open-framework gravel can cause adjacent sand layers to migrate into their large voids, through suffusion and contact erosion, creating local collapse zones. The settlement of the soil column above causes the appearance of sinkholes on the soil surface. Contact erosion is selective here, contrary to what is classically considered (Bonelli, 2012; Bonelli, 2013): only the sand of the sandy gravel is eroded by the flow in the open-framework gravel. In addition, the appearance of an open-framework gravel zone within the sandy-gravel layer, at the level of the decrease in the thickness of this layer can induce a surface signature. The flow can then be locally fast enough to initiate contact erosion of the sandy-marly support layer, which can also lead to settlement and the appearance of a sinkhole on the soil surface.

It is important to note that these sinkholes can occur without the prior appearance of sand boils, contrary to what is often assumed (Zwanenburg et al., 2018; Tourment et al., 2018; Van et al., 2022).

5.2 The four basic situations explaining erosion signatures

The two main hazards of a risk analysis are flooding by rising water table and flooding by dike breach. Four basic situations can be defined according to the presence or absence of a topsoil, and the presence or absence of a paleochannel. These four basic situations explain the origin and distribution of internal erosion signatures in the floodplain protected by river dikes, in the case of a dike located on a paleovalley fill consisting of sandy gravel (Figure 11). This general framework is deduced from the results of numerical simulations (Deng et al., 2025; Bonelli and Girolami, 2025).

In the absence of topsoil (cases A and B), the water table rises during a flood above the ground surface, causing the flooding of the protected area by groundwater. The uplift condition corresponds to the critical hydraulic gradient of Terzaghi and causes the fluidization of the sand at the dike toe (also known as heave and blowout, that is to say the uplift of the grains of a non-cohesive soil). The development of an open-framework gravel pipe under the embankment can initiate a localized erosion zone at the dike toe, and cause the appearance of a sinkhole. An thorough analysis by numerical modelling is necessary to provide orders of magnitude and clarify the influence of the presence of a paleochannel. When there is no topsoil, there is no sand boil, and the most likely location for a sinkhole is the dike toe.

If a low-permeability topsoil layer covers the sandy gravel, and there is no paleochannel (case C), the entire sandy gravel layer is saturated and under pressure. If a defect in the topsoil layer causes a leak to appear and triggers erosion, a sand boil may appear, and possibly a sinkhole linked to this sand boil. This can occur anywhere between the dike and the end of the sandy gravel layer, but the most likely location is the place where the artesian pressure is highest, at the dike toe. The flow is confined in the 2D plane perpendicular to the embankment, and the 3D effect probably becomes very important. An thorough analysis using numerical modelling is needed to provide orders of magnitude and clarify the influence of the 3D effect.

If a low-permeability topsoil layer covers the sandy gravel, and there is a paleochannel (case D), the upper part of the sandy gravel is likely to be subjected to significant groundwater flow. If a defect in the topsoil layer causes a leak to appear and triggers erosion, a sand boil may appear, and possibly a sinkhole linked to this sand boil. This can appear anywhere from the dike toe and over a distance that can only be assessed by numerical modeling, but the two most likely location are the dike toe, and the reduction in thickness of the sandy gravel layer, i.e. the entrance area of the paleochannel.

An important result for case D is to be confirmed by numerical modeling: in the absence of a defect in the topsoil layer (no leakage or sand boil), the appearance of open-framework gravels can cause erosion of the surrounding soils (sandy gravels, sand or sandy marls) and induce a sinkhole. Two most likely locations are the dike toe, and the entrance area of the paleochannel.

6 Conclusion

When analyzing the flood risk of a floodplain protected by existing river dikes, it is essential to understand the causes of surface signatures (leaks, sand boils, sinkholes) observed during and immediately after the river flood. The conclusion of this study is that the distribution of these signatures is directly related to the shape and dimensions of the paleovalley and paleochannels, and to the presence of a low-permeability topsoil.

The key point is the multi-scale and multidisciplinary charactere of the methodology. The description of the morphological organization and stratigraphic architecture of the river and its alluvial plain constitutes the first step, at large spatial scales. The observation of the subsoils supporting the dike system constitutes the second step. This involves locating, using geophysical methods, the interfaces between the paleovalley and the paleochannels, as well as the low-permeability supporting soils. The correlation between the geophysical observables (e.g. electrical resistivity) and the quantities of geomechanical interest (hydraulic conductivity) requires information on existing soils, most often obtained locally with geotechnical methods (e.g. by coring). The analysis of scenarios showing the influence of the shape of the paleovalley and paleochannels on the location and development of internal erosion is the third step.

This methodology has been applied to the study area of the Agly dike system, where numerous leaks, sand boils and sinkholes were observed. The combined use of FDEM and ERT methods proves to be a fast and cost-effective solution to continuously map the subsurface and capture shallow horizontal information. In the case of a permeable layer consisting of sandy gravel, the classical backward erosion piping scheme is not relevant to explain the observed sand boils, since they are mainly caused by a backward erosion suffusion process. Both suffusion and contact erosion appear to be the origin of the sinkholes.

Declaration of Competing Interest

The authors declare that they have no known competing financial interests or personal relationships that could have appeared to influence the work reported in this article.

Fundings

This research was supported by the Water departement of INRAE (Aqua department, Pari Scientifique), by the Region Centre-Val de Loire (contribution of Academic Initiative Project RHEFLEXES/201900134935), by Aix-Marseille University (ECCOREV/ITEM 2023 PALERO Project Relationships between paleo-channels and internal erosion processes around protective dikes), by the Directorate General for Risk Prevention (DGPR) and by the Water and Environment INRAE Carnot Institute.

Acknowledgments

We thank the managers of the Agly river dikes (SMBVA, F. Nicoleau) for having provided authorizations of this work and for fruitful discussions. We thank the compagny DRIM for ERT results on P1 and P3 profiles, as part of a service order on behalf of INRAE. We thank the company Naga Geophysics for ERT results (raw data) on P2, P4, P6, P7 profiles, as part of a service order on behalf of INRAE.

References

Amin A., Girolami L., Risso F. (2021) On the fluidization/sedimentation velocity of a homogeneous suspension in a low-inertia fluid, *Powder Technology* **391**, 1-10.

Aunay B. (2007) Apport de la stratigraphie séquentielle à la gestion et à la modélisation des ressources en eau des aquifères côtiers. PhD, Université Montpellier II, 371 p.

van Beek V. M., Knoeff H., Sellmeijer H. (2011) Observations on the process of backward erosion piping in small-, medium-and full-scale experiments, *European Journal of Environmental and Civil Engineering* **15**(8), 1115-113.

Blanchy G., Saneiyan S., Boyd J., Mc Lachlan P., Binley A. (2020) ResIPy, an intuitive open source software for complex geoelectrical inversion/modeling, *Computers & Geosciences* **137**, 104423.

Bonelli S., Girolami L., Internal erosion of sandy gravel and occurrence of open-framework gravels in the subsoil of a river dike, preprint submitted, 2025.

Bonelli S. (2012) *Erosion of Geomaterials*, (Ed), John Wiley & Sons, 372 p.

Bonelli S. (2013) *Erosion in Geomechanics Applied to Dams and Levees*, (Ed), Wiley/ISTE, 388 p.

Calvet M. (1996) Morphogenèse d'une montagne méditerranéenne : les Pyrénées orientales. BRGM, Document no125, Presse Universitaire de Perpignan, 3 tomes, BRGM, Orléans.

Camici S., Barbetta S., Moramarco, T. (2017) Levee body vulnerability to seepage: the case study of the levee failure along the Foenna stream on 1 January 2006 (central Italy), *Journal of Flood Risk Management* **10**(3), 314-325.

Carozza J.-M., Puig C. (2011) Changements environnementaux, vulnérabilité et adaptation des sociétés du passé : exemple du Petit Age Glaciaire en Roussillon (xiiie-xvie s.), *Sud-Ouest Européen* **32**, 67-79.

Carozza J.-M., Puig C., Odiot T., Passarrius O., Valette P. (2013) L'édification de la Basse Plaine de la Salanque (Roussillon, France) au cours de la seconde partie de l'holocène et ses implications sur la répartition des sites archéologiques, *Quaternaire* **2**, 129-139.

Carozza J.-M. (2015) Synthèse des connaissances géomorphologiques et géoarchéologiques autour de l'Agly : aide à la décision en vue des travaux de réaménagement des digues, Rapport Conseil Départemental des Pyrénées-Orientales, Pôle Archéologie, 26 p.

Ceccato F., Simonini P. (2023) The effect of heterogeneities and small cavities on levee failures: The case study of the Panaro levee breach (Italy) on 6 December 2020. *Journal of Flood Risk Management* **16**(2), e12882.

CIRIA. *The International Levee Handbook,* London, UK, 2013.

Chavez Olalla J., Winkels T.G., Ngan-Tillard D.J.M., Heimovaara T.J. (2022) Geophysical tomography as a tool to estimate the geometry of soil layers: relevance for the reliability assessment of dikes, *GEORISK* **16**(4), 678–698.

Clauzon G. (1990) Restitution de l'évolution géodynamique néogène du bassin du Roussillon et de l'unité adjacente des Corbières d'après les données écostratigraphiques et paléogéographiques, *Paléobiologie Continentale* **17**, 125-155.

Dahlin T. (2001) The development of DC resistivity imaging techniques, *Computers & Geosciences* **27**(9), 1019-1029.

Dalrymple R.W., Boyd R., Zaitlin B.A., Incised Valley Systems: Origins and Sedimentary Sequences, *SEPM Spec. Publ.* **51**, 1994.

Deng Z., Benahmed N., Girolami L., Philippe P., Bonelli S., Wang G., Numerical investigation of internal erosion mechanisms regarding stratigraphy: Agly dike case study, preprint submitted, 2025.

Dezert T., Fargier Y., Palma Lopes S., Côte P. (2019) Geophysical and geotechnical methods for fluvial levee: a review, *Engineering Geology* **260**.

Duvail C., Le Strat P., Bourgine B. (2001) Atlas géologique des formations plio-quaternaires de la plaine du Roussillon (Pyrénées-orientales), Rapport BRGM, RP-51197-FR, 45 p.

Duvail C. (2008) Expression des facteurs régionaux et locaux dans l'enregistrement sédimentaire d'une marge passive. Exemple de la marge du Golfe du Lion, étudiée selon un continuum terre-mer, PhD, Univ. Montpellier, 261 p.

Fell R., MacGregor P., Stapledon D., Bell G., Foster M., 2014. *Geotechnical Engineering of Dams*, 2nd Edition. 419 ed. CRC Press.

Friend P. F., Slater M. J., Williams R. C. (1979) Vertical and lateral building of river sandstone bodies, Ebro Basin, Spain, *Journal of the Geological Society* **136**(1), 39–46.

Girolami L., Bonelli S., Valois R., Chaouch N., Burgat J. (2023) On Internal Erosion of the Pervious Foundation of Flood Protection Dikes, *Water* **15**(21), 3747.

Julinek T., Duchan D., Riha J. (2020). Mapping of uplift hazard due to rising groundwater level during floods, *Journal of Flood Risk Management* **13**:e12601.

Kolb C.R. (1975) Geologic Control of Sand Boils Along Mississippi River levees. USACE Vicksburg, Report S-75-22, 35 p.

Labaune C., Tesson M., Gensous B., Parize O., Imbert P., Delhaye-Prat V. (2010) Detailed architecture of a compound incised valley system and correlation with forced regressive wedges: Example of Late Quaternary Têt and Agly rivers, western Gulf of Lions, Mediterranean Sea, France, *Sedimentary Geology* **223**, 3–4, 360-379.

Li Y., Craven J., Schweig E.S., Obermeier S.F. (1996) Sand boils induced by the 1993 Mississippi River flood: Could they one day be misinterpreted as earthquake-induced liquefaction?, *Geology* **24**(2), 171-174.

Lunt I.A., Bridge J.S. (2007) Formation and preservation of openframework gravel strata in unidirectional flows, *Sedimentology* **54**:71–87.

Luo Y., Huang Y. (2020) Effect of open-framework gravel on suffusion in sandy gravel alluvium, *Acta Geotechnica* **15**:2649–2664.

Marchi M., Martinez M.F.G., Gottardi G., Tonni G.L. (2021) Field measurements on a large natural sand boil along the river Po, Italy. *Quarterly Journal of Engineering Geology and Hydrogeology* **54**(4), qjegh2020-097.

Miall A.D. (1996) The Geology of Fluvial Deposits: Sedimentary Facies, Basin Analysis, and Petroleum Geology, Springer, 598 p.

Michelazzo G., Paris E., Solari L. (2018), On the vulnerability of river levees induced by seepage, *Journal of Flood Risk Management* S677–S686.

Morton L.W., Olson K.P. (2015) Sinkholes and sand boils during 2011 record flooding in Cairo, Illinois, *Journal of Soil and Water Conservation* **70**(3), 49A-54A.

Mouhri A., Flipo N., Rejiba F., de Fouquet C., Bodet L., Kurtulus B., Tallec G., Durand V., Jost A., Ansart P., Goblet P. (2013) Designing a multi-scale sampling system of stream-aquifer interfaces in a sedimentary basin, *Journal of Hydrology* **504**, 194-206.

Pazzi V., Di Filippo M., Di Nezzac M., Carlà T., Bardi F., Marini F., Fontanelli K., Intrieri E., Fanti R., Integrated geophysical survey in a sinkhole-prone area: Microgravity, electrical resistivity tomographies, and seismic noise measurements to delimit its extension, *Engineering Geology* **243** (2018) 282–293.

Rabineau M. (2001) Un modèle géométrique et stratigraphique des séquences de dépôt quaternaires sur la marge du Golfe du Lion : enregistrement des cycles climatiques de 100 000 ans, PhD, Univ. Rennes I, 455 p.

Semmens S.N., Zhou W. (2019) Evaluation of environmental predictors for sand boil formation: Rhine–Meuse Delta, Netherlands, *Env. Earth Sci.* **78**, 1-11.

Tesson M., Labaune C., Gensous B. (2005) Small rivers contribution to the Quaternary evolution of a Mediterranean littoral system: The western gulf of Lion, France, *Marine Geology* **222** (223), 313-334.

Tourment R., Benahmed N., Nicaise S., Mériaux P., Salmi A., Rougé M. (2018) Lessons learned on the damaged on the levees of the Agly River, analysis of the sand boils phenomena, Proc. of the 26th ICOLD Congress, Q.103 R.21, Vienna.

USBR, Best Practices in Dam and Levee Safety Risk Analysis, Bureau of Reclamation & US Army Corps of Engineers. Dam Safety Office. Security, Safety and Law Enforcement Office, 2019, 1337 p.

Valois R., Camerlynck C., Dhemaied A., Guerin R., Hovhannissian G., Plagnes V., Rejiba F., Robain H. (2011) Assessment of doline geometry using geophysics on the Quercy plateau karst (South France), *Earth surface processes and landforms* **36**(9), 1183-1192.

Van M.A., Rosenbrand E., Tourment R., Smith P., Zwanenburg C. (2022) Failure paths for levees, International Society of Soil Mechanics and Geotechnical Engineering (ISSMGE), TC201.

Wang R., Colombera L., Mountney N.P. (2019) Geological controls on the geometry of incised-valley fills : Insights from a global dataset of Late Quaternary example, *Sedimentology* **66**(6), 2134-2168.

Wolff T. F. (2002) Performance of levee underseepage controls: A critical review. Rep. No. ERDC/GSL TR-02-19. Washington, DC: USACE.

Zwanenburg C., López-Acosta N.P., Tourment R., Tarantino A., Pozzato A., Pinto A. (2018) Lessons Learned from Dike Failures in Recent Decades. *International Journal of Geoengineering Case Histories*, **4**(3), 203-229.

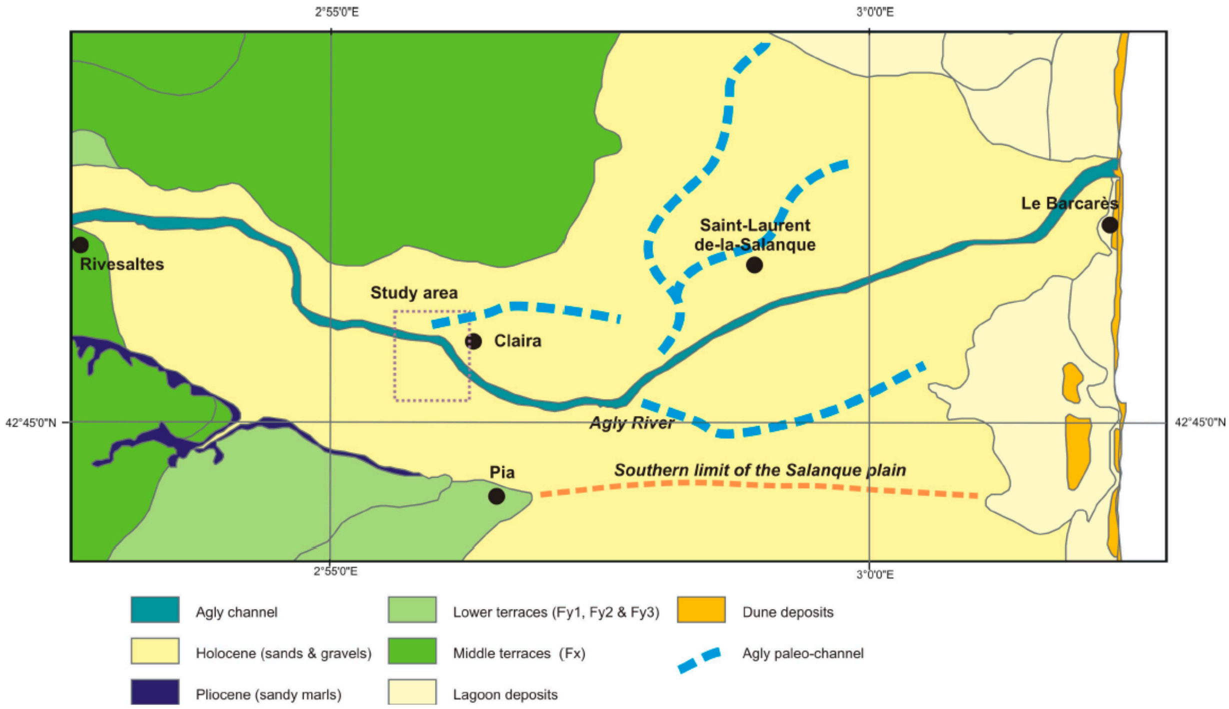

Figure 1. Geological organisation of the Salanque alluvial plain, modified from Fonteilles et al. (1993) and Carozza et al. (2013). The study area is located approximately 8 km from the sea, upstream the town of Claira.

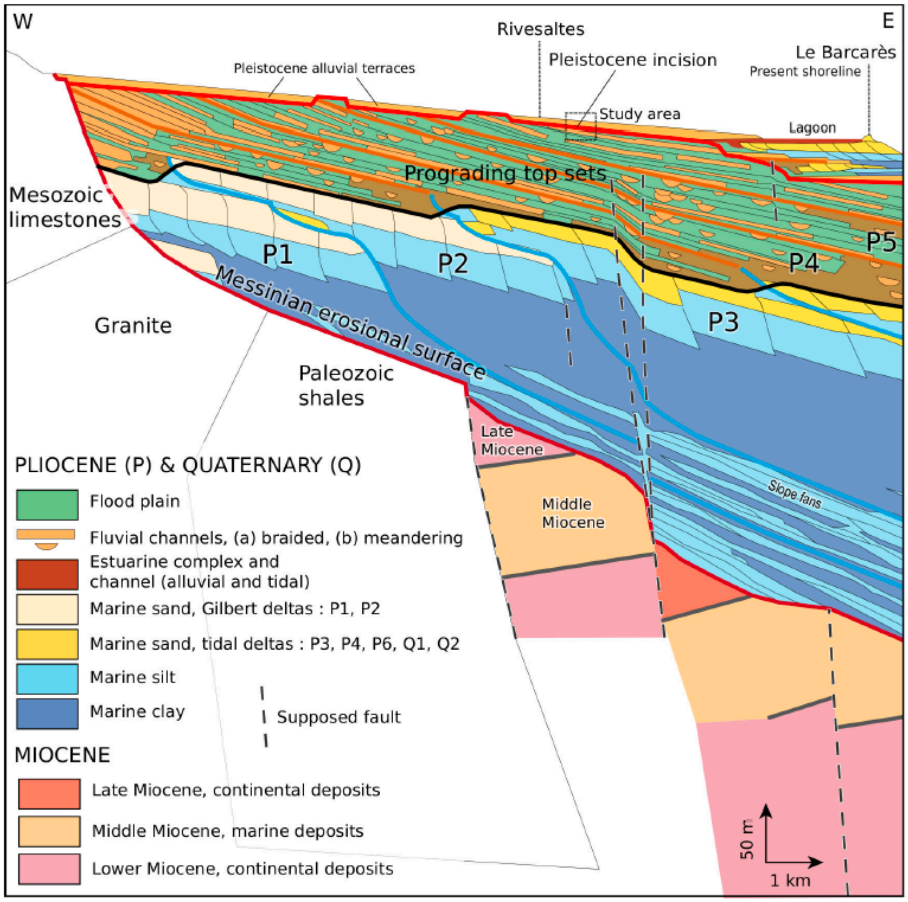

Figure 2. Section of the Salanque plain highlighting the basal incision of the impermeable Pliocene substrate which forms a palo-valley filled by very permeable Holocene alluvial sediments. The profile of the Agly channel is shown upstream and downstream of the study area, located northwest of Claira.

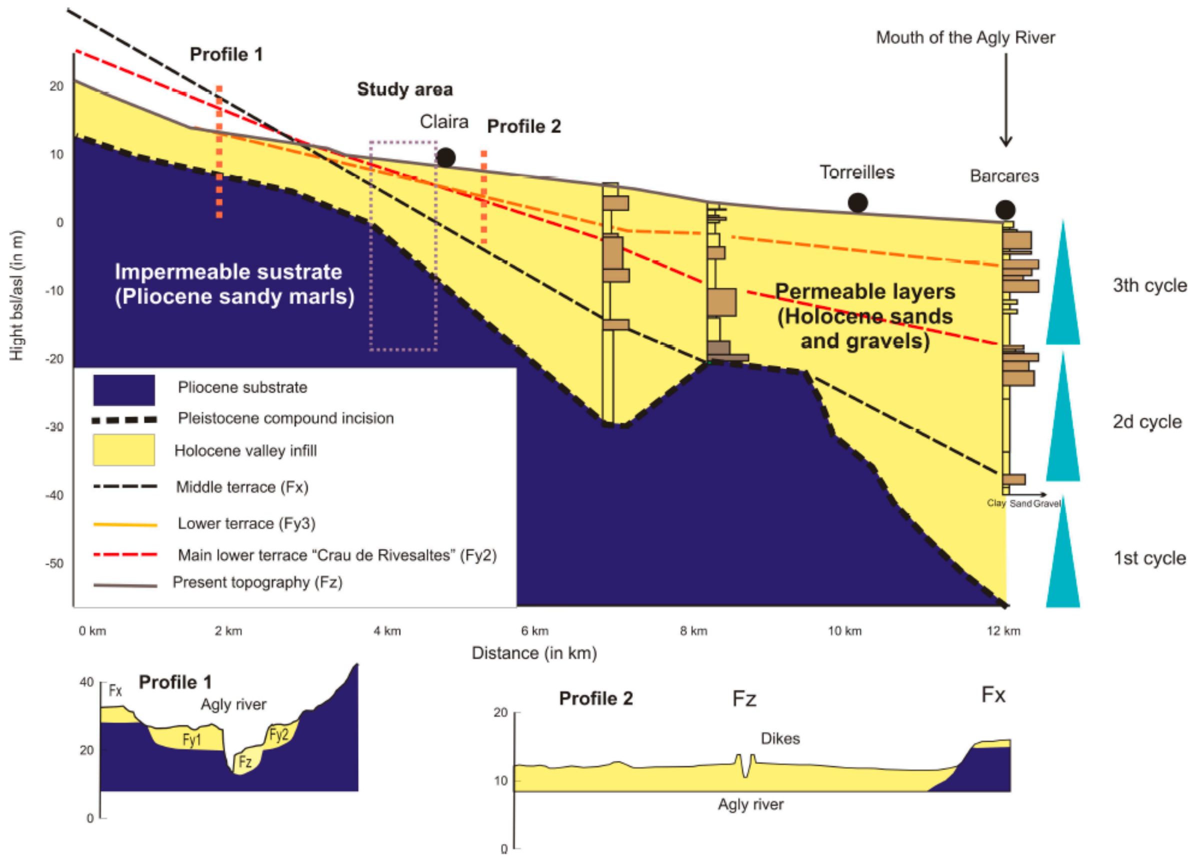

Figure 3. Schematic scross-section of the Salanque alluvial plain, adapted and modified from Carozza (2018). The profile of the Agly channel is shown upstream and downstream of the study area, located northwest of Claira. Sediment cores are shown in the valley (Tesson et al., 2005).

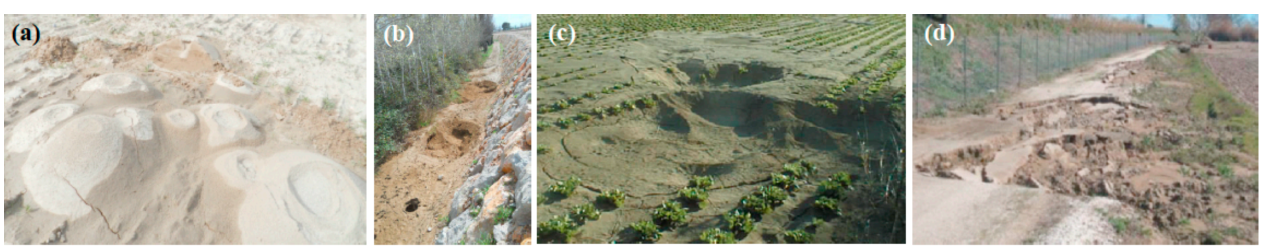

Figure 4. Erosion signatures observed in the floodplain of the Agly dikes (Pyrénées-Orientales, France) after flood events : sand boils (a), sinkholes (b,c, d). Pictures made in 2012, 2013, and 2014 (INRAE).

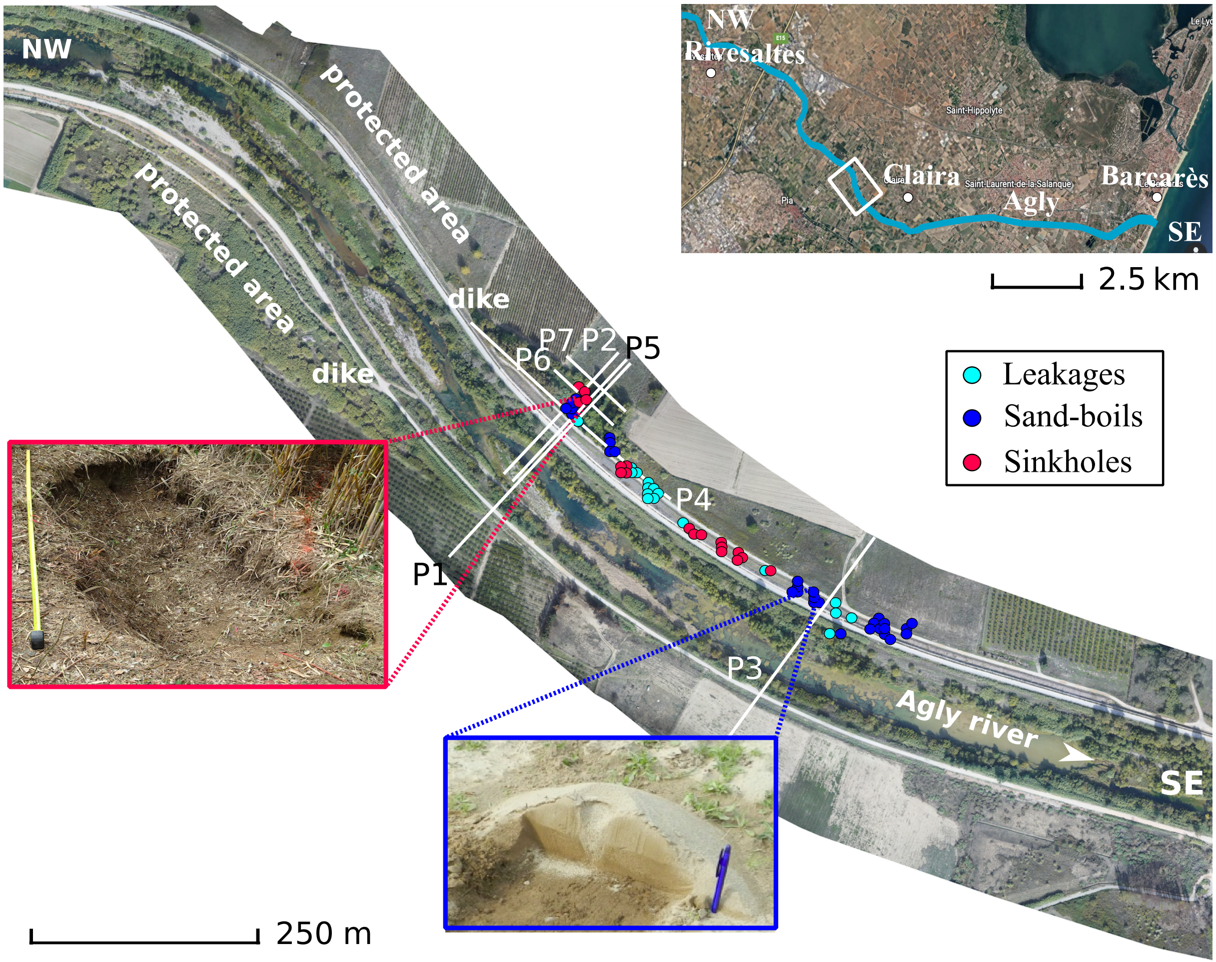

Figure 5. Presentation of the study area : the diked riverbed and the protected plains bordering it, on which erosion signatures (leaks, sand boils, sinkholes) observed on the North bank after the flood event of March 6, 2013 were reported. The white lines represent the position of the electrical profiles (ERT) exposed in this study. Examples of sinkholes and sand boils observed along the profiles are illustrated (INRAE pictures made in 2022 and 2013).

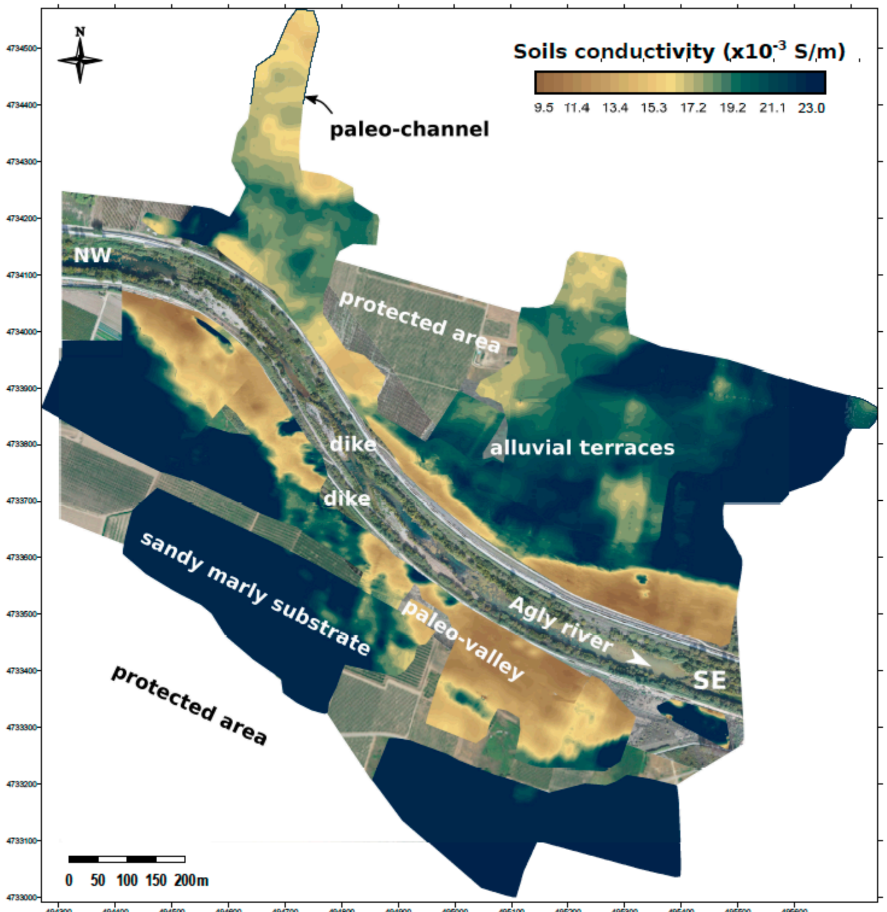

Figure 6. FDEM surface map of the soils electrical conductivity averaged on the first 6 meters of depth of the study area. The erosion signatures of March 6, 2013 are also reported on this map.

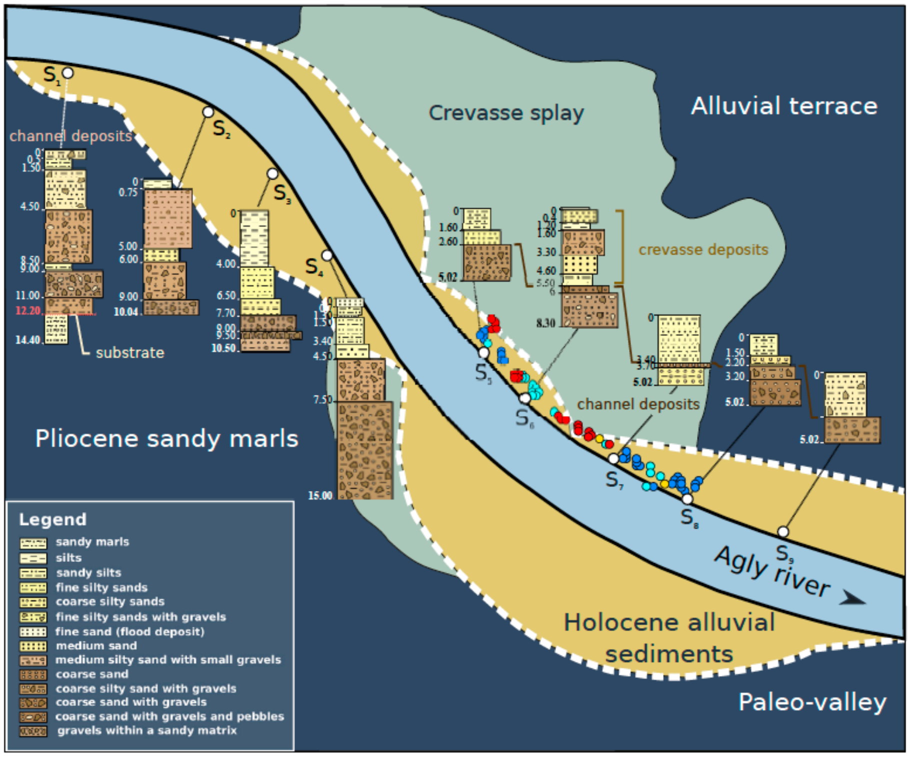

Figure 7. Interpretation of the FDEM surface map obtained from geomorphological analyses and sedimentary boreholes sampled in the study area (S1–9). The erosion signatures (leaks, sand boils, sinkholes) observed on the North bank after the flood of March 6, 2013 are represented respectively in dark blue, light blue, and red (North orientation and color scale are indicated in Figure 6).

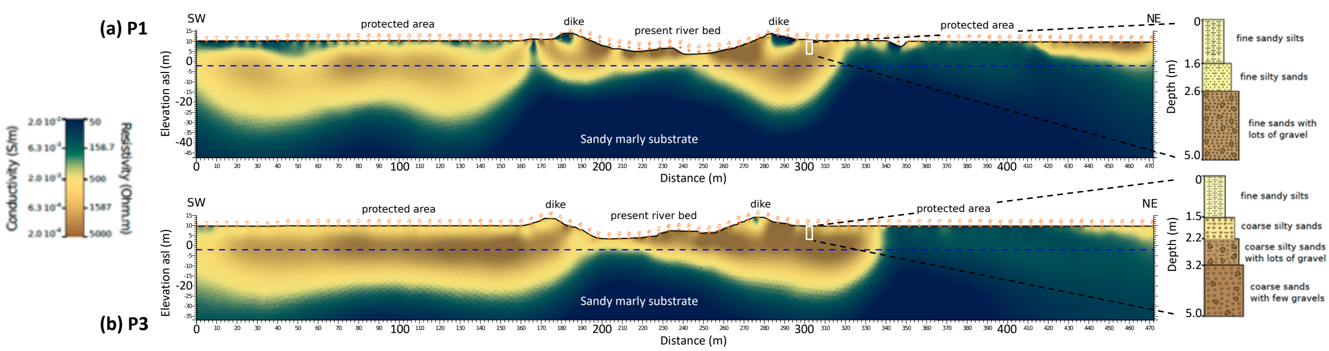

Figure 8. Vertical section of soil resistivity along profiles P1 (a) and P3 (b) and 5-meter-thick soil cores taken near the dike toe, in front of the berm. Profiles P1 and P3 across the whole diked bed where sand boils and sinkholes where reported on the North bank after the flood of March 6, 2013.

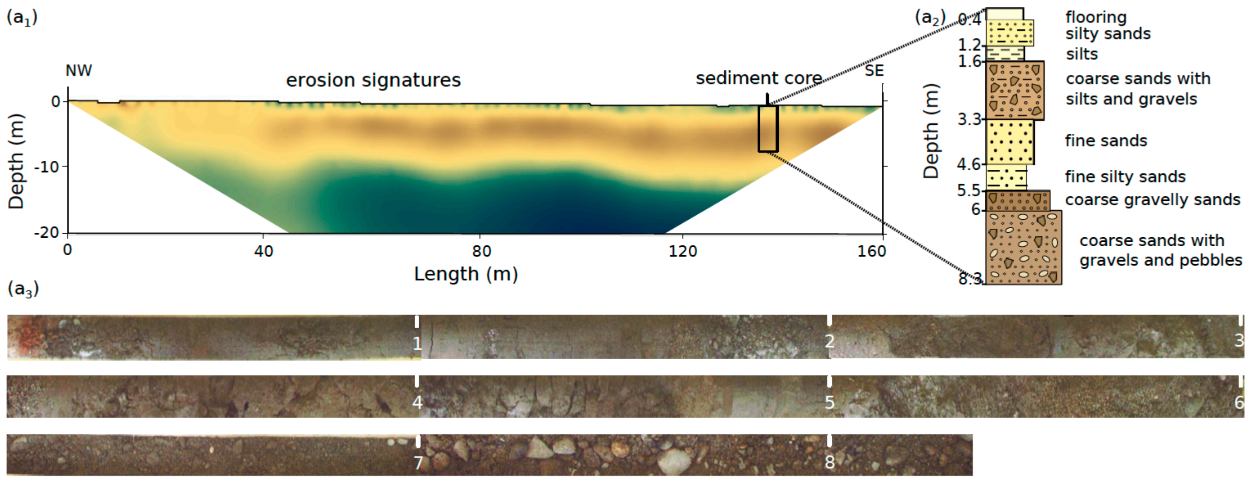

Figure 9. (a1) Vertical section of soil conductivity/resistivity along profile P4, near and along the North dike where leaks, sand boils, and sinkholes where reported in 2013. (a2) 8.30 meters thick sediment core taken near the dike toe, in front of the berm. (a3) Picture of the sediment sample (from the surface, upper left, to the base, lower right). The color scale is shown in Figure 8.

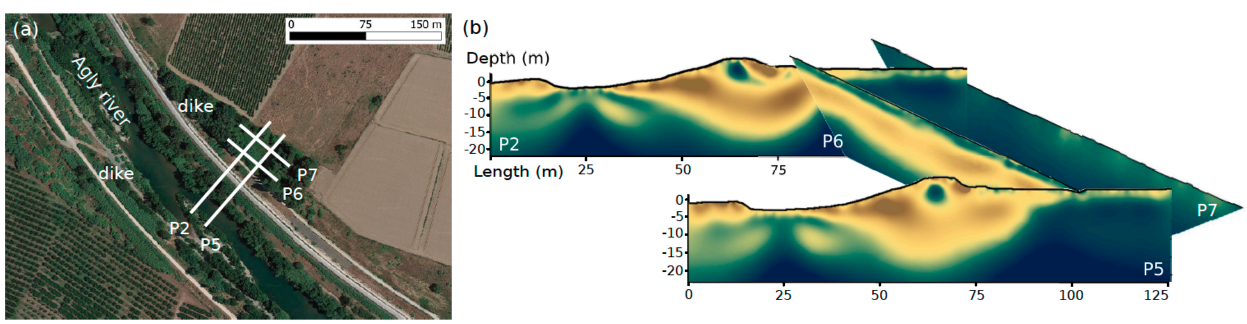

Figure 10. (a) Location and layout of four vertical soil conductivity/resistivity sections taken along the North bank (along profiles P2, P5, P6, P7) where sand boils and sinkholes were reported in 2013; (b) Vertical soil conductivity/resistivity section along these profiles (P2,P5, P6, P7). The color scale is shown in Figure 8.

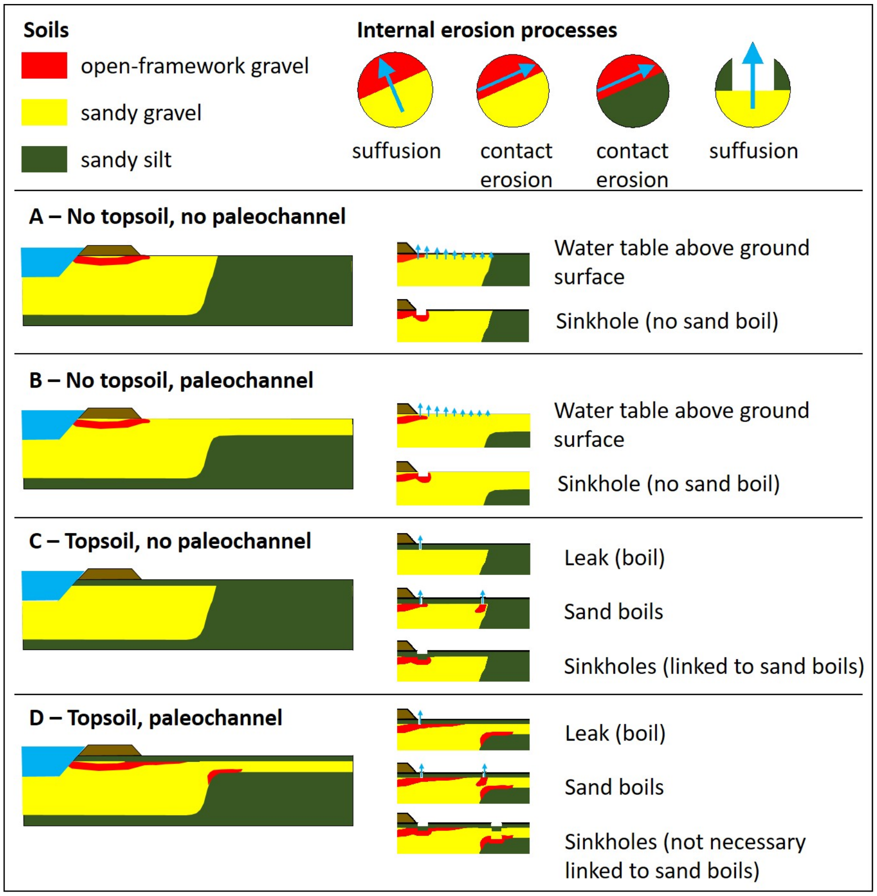

Figure 11. The four basic situations explaining the origin and distribution of erosion signatures in the floodplain protected by river dikes. Case of a dike built on a paleovalley made up of sandy gravel. On the left, development of open-framework gravelly zones (red), no defects in the topsoil layer (no sand boils). On the right, typology of appearance of the three surface signatures: leaks, sand boils and sinkholes. The two influencing parameters are the presence of a topsoil and the presence of a paleochannel.